The physical basis of mineral optics
I. Classical theory

R. G. J. STRENS AND ROBERT FREER

School of Physics, The University, Newcastle upon Tyne NE1 7RU

SUMMARY. The Helmholtz dispersion equations have been rewritten in a form that enables the optical constants of both transparent and opaque media to be calculated from their spectra. Both Helmholtz equations are used to describe the optical properties of opaque media, and to obtain values of reflectance, refractive index, and absorption coefficient. The Sellmeier dispersion equation is a special case of the dispersive Helmholtz equation applicable to weakly absorbing media (including the great majority of minerals studied in thin section): it is used to derive the wavelength-, composition-, direction-, and volume-dependence of the principal indices in mixed crystals of monoclinic or higher symmetry. The treatment can be extended to triclinic crystals.

The birefringence of transparent phases is the expression in the visible region of the pleochroism of absorption bands in the ultra-violet. The bireflectance of opaque phases depends also upon the pleochroism of bands in the visible and near infra-red, resulting in extreme sensitivity of the optics of opaque materials to changes in wavelength, composition, and structure. The optical anisotropy of both transparent and opaque phases may be calculated if the dependence of the spectra on structure can be established by measurement or by calculation from structure data. The quantitative application of Bragg's method is restricted to phases of very simple chemistry and structure (e.g. calcite and rutile), but it may be applied qualitatively to rationalize the optic orientations of phases containing only closed-shell ions of neon or argon configuration, including many pyroxenes, amphiboles, micas, and chain aluminosilicates. When open-shell (transition metal) ions enter the structure, the general rule is that the anisotropy becomes more closely related to the distortion of the coordination polyhedron about the metal ion, and for ions of formal charge $\geqslant 3$, this source of anisotropy is usually dominant.

A better understanding of mineral optics will require much more work on the ultra-violet spectra of common transparent minerals, with particular emphasis on establishing the dependence of absorption band wavelengths, widths, and absorbances on interatomic distance and other structural variables. For opaque minerals, the need is for more accurate data spanning a wider range of wavelengths, and for improved methods of representing the data, such as plots in the ε_1–ε_2 plane.

THE aim of this paper is to provide a theoretical framework within which the optical properties of chemically and structurally complex media, both opaque and non-opaque, may be discussed quantitatively. Three points have been kept in mind. First, the theory should have a sound physical basis. Secondly, it should enable the optical properties to be calculated with an accuracy comparable with that of the experimental data. Thirdly, the mathematical content should not be such as to render it inaccessible to the working mineralogist, which restricts us to phenomenological equations such as those of Helmholtz or Lorenz and Lorentz. These equations have been slightly modified by Drude's electromagnetic theory of dispersion, and by the application of quantum theory, but their form has not changed. A comprehensive review of the development of physicochemical optics since the earliest times (including the development of the Helmholtz, Lorenz–Lorentz, and Drude equations) has been given by Partington (1953), and his review together with Jenkins and White (1976) is the source of our equations 1 to 3.

The variation of index with wavelength is described by dispersion equations, of which the most useful are the purely mechanical equations of Helmholtz, and a modification of the Lorenz–Lorentz equation that treats the medium as an assemblage of polarizable particles. Both contain terms depending on the number of oscillators or polarizable particles in unit volume, and they are therefore capable of describing the composition- and volume-dependence of indices at constant wavelength, and the wavelength-dependence at constant volume and composition. The dependence of index on direction and crystal structure (optical anisotropy) is also implicit in the dispersion equations. The Helmholtz equations relate the index to the wavelengths, widths, and absorbances of absorption bands in the spectrum of the medium, so that optical anisotropy in the visible region may be seen as the expression of pleochroism in the ultra-violet and infra-red. The Lorenz–Lorentz equation relates index to polarizability, and the polarizabilities themselves depend on the wave-

lengths and absorbances of the absorption bands. The difference between the Helmholtz and Lorenz–Lorentz equations lies in the treatment of the internal field in dielectrics (insulating media).

The Lorenz–Lorentz equation is in theory the more satisfactory, but it is often difficult or impossible to apply in practice for two reasons. First, the polarizability tensor of an ion occupying a general position in the unit cell has at least as many different non-zero elements (p) as the crystal has principal indices and extinction angles. The pq elements of the q ionic polarizability tensors (which describe the variation of polarizability with direction) are uniquely related to the p observable principal indices and extinction angles only if the number of inequivalent atoms in the unit cell is $q = 1$. If $q > 1$, then $p(q-1)$ constraints must be applied to force a solution. These constraints may be supplied by the presence of some ions in special positions of higher symmetry, or by making approximations, e.g. that some ions have negligible polarizability, but until polarizabilities can be calculated from structure data the application of the Lorenz–Lorentz equation will be restricted to chemically and structurally simple phases with no more than two or three ions (e.g. TiO_2, $CaCO_3$). A second problem is that the equation is applicable only to dielectrics in which the interatomic distance is large compared with the sum of the atomic radii, i.e. those in which overlap is negligible (see Mott and Gurney, 1964, pp. 10–19). It cannot form the basis of an approach that is intended to treat both opaque and non-opaque media of considerable chemical and structural complexity. We have therefore reconsidered the applications of the relatively neglected Helmholtz equations as modified by Drude's electromagnetic theory of dispersion and by the application of quantum theory.

The Helmholtz equations

The Helmholtz equations were originally based on a mechanical analogy for the interaction between the alternating electric field associated with the light wave and the bound electrons of the medium. The analogy is that of the driven damped one-dimensional oscillator. A simple example is that of an oscillator comprising a mass m on a spring of force constant k, having a natural frequency $\omega = (k/m)^{\frac{1}{2}}$, and driven by moving the hand. The damping is provided by the hysteresis of the spring. If the forcing frequency is low compared with ω, the motion of the mass follows that of the hand with a small phase lag: if it is high, there is little movement of the mass. Both cases involve only slight absorption of energy by the oscillator, and correspond to values of the refractive index near 1, accompanied by small dispersion and absorption. Only when the forcing frequency approaches the resonant frequency ω is energy strongly absorbed, resulting in rapid variation of index, dispersion, and absorption with frequency, and also rapid changes in the phase relation between excitation and response. The frequency range over which resonance occurs (which determines the rate of change of index, dispersion, absorption, and phase angle) increases with damping. For more detailed discussions of the subject see Jenkins and White (1976). The mechanical analogy proved very successful and led to the development of the Sellmeier and Helmholtz dispersion equations, besides demonstrating in an easily understandable way the intimate relations between absorption, dispersion, and refraction, and the dependence of these quantities on the frequency, width, and absorbance of bands in the spectra of the medium considered.

Symbols used in equations (numbers are those of equations in which symbol first appears).

A	constant in Helmholtz and Sellmeier equations (1)	a_i	linear absorption coefficient at band maximum (4)
I	integrated absorbance (3)	a, b	constants in equation (7)
L	$\lambda^2/(\lambda^2 - \lambda_i^2)$ (follows 6b)	$\mathbf{a, b}$	constants in equation (8)
M	molar refractivity (12)	c_i	form factor of absorption band (4)
N	number of oscillators in volume V (2)	c	velocity of light in vacuum (2)
R	specular reflectance at normal incidence (10)	e	electronic charge (2)
V	molar volume (2)	f_i	oscillator strength of absorption band (2)
α	polarizability (where context implies) (11)	i	$\sqrt{(-1)}$
ε	complex dielectric constant (1)	k	dimensionless absorption coefficient (1)
φ	extinction angle on (010) (8)	m	mass of electron (2)
θ	a phase angle (8)	n	principal refractive index (mean $\bar{n}$, general direction n') (1)
λ	wavelength of observation (1)		
λ_i	wavelength of absorption band maximum (1)	r	an interatomic distance (11)
μ	refractive index of immersion medium (10)	w_i	full width of absorption band at half height (1)
η	specific refractivity (13)	x	compositional variable, $0 \leqslant x \leqslant 1$ (7)
$\mathbf{N}$	complex refractive index (10)		

The Helmholtz dispersion equations relate the real (ε_1) and imaginary (ε_2) parts of the complex dielectric function ($\varepsilon = \varepsilon_1 + i\varepsilon_2$) to the wavelength of observation (λ), and the wavelengths (λ_i), widths (w_i), and absorbances (A_i) of bands in the absorption spectrum of the medium considered:

$$\varepsilon_1 = n^2 - k^2$$

$$= 1 + \sum \frac{A_i \lambda^2}{\lambda^2 - \lambda_i^2 + w_i^2 \lambda^2/(\lambda^2 - \lambda_i^2)} \quad (1a)$$

$$\varepsilon_2 = 2nk$$

$$= \sum \frac{A_i w_i \lambda^3}{(\lambda^2 - \lambda_i^2)^2 + w_i^2 \lambda^2}. \quad (1b)$$

Here, n is the refractive index for the polarization considered, and $k = a\lambda/4\pi$ is the dimensionless absorption coefficient, a being the linear absorption coefficient to base e. Drude's dispersion theory, modified to allow for oscillator strengths (f) less than unity (which are permitted by quantum theory), assigns to A_i the value:

$$A_i = \frac{N}{V} \frac{e^2}{\pi m c^2} f_i \quad (2)$$

where N is the number of oscillators in the volume V. The oscillator strength $0 \leqslant f_i \leqslant 1$ is related to the integrated absorbance of the band by:

$$f_i = \frac{V}{N} \frac{mc^2}{\pi e^2} I_i \quad (3)$$

(Robbins and Strens, 1972) where I_i is conveniently stated in the form:

$$I_i = c_i a_i w_i. \quad (4)$$

Here, a_i is the linear absorption coefficient at band maximum, w_i is the full width at half height (expressed as $\Delta\lambda$ and not in wave numbers), and c_i is the form factor, which is $(\pi/2)^{\frac{1}{2}}$ for a Gaussian band, and $\pi/2$ for a Lorentzian. The Helmholtz equation assumes a Lorentzian band shape, and in the interests of mathematical consistency we take $c_i = \pi/2$, although many absorption bands in and near the visible region are more nearly Gaussian. Substituting (2), (3), and (4) into (1a) and (1b), we have:

$$\varepsilon_1 = n^2 - k^2$$

$$= 1 + \frac{1}{2\pi} \sum \frac{a_i w_i \lambda^2}{(\lambda^2 - \lambda_i^2) + w_i^2 \lambda^2/(\lambda^2 - \lambda_i^2)} \quad (5a)$$

$$\varepsilon_2 = 2nk$$

$$= \frac{1}{2\pi} \sum \frac{a_i w_i^2 \lambda^3}{(\lambda^2 - \lambda_i^2)^2 + w_i^2 \lambda^2}. \quad (5b)$$

These equations provide the required link between the absorption spectra and the optical properties of both opaque and transparent media.

Optics of transparent media

Transparent media are those in which there are no strong absorption bands near the visible region, i.e. $(\lambda - \lambda_i)/w_i$ is large, and $k \to 0$. The second Helmholtz equation (5b) may be ignored because $2nk \to 0$. The first Helmholtz equation (5a) simplifies considerably, for with w_i small compared with λ_i, and λ_i small compared with λ, the k^2 and $w_i^2 \lambda^2/(\lambda^2 - \lambda_i^2)$ terms may be neglected, yielding the Sellmeier dispersion equation:

$$n^2 = 1 + \sum \frac{A_i \lambda^2}{\lambda^2 - \lambda_i^2}. \quad (6a)$$

In a region far from any absorption band, the precise shape and width of the band has little influence on the optical properties, and the equation may be written in terms of $(\lambda, \lambda_i, I_i)$ rather than $(\lambda, \lambda_i, c_i a_i w_i)$:

$$n^2 = 1 + \frac{1}{\pi^2} \sum \frac{I_i \lambda^2}{\lambda^2 - \lambda_i^2}. \quad (6b)$$

Sellmeier's A is then given by $A_i = I_i/\pi^2$, and if we write $L = \lambda^2/(\lambda^2 - \lambda_i^2)$, the equation has the very simple form $n^2 = 1 + IL/\pi^2$. This equation may be applied to obtain I_i and λ_i if the refractive index is known at two wavelengths, and if the dispersion is dominated by a single band (or several bands spaced closely compared with $\lambda - \lambda_i$). The resulting λ_i give an indication of the optically significant transition energies, and the dependence of these energies on composition, structure, and volume. In compounds of the common closed-shell ions (O^{2-}, F^-, Na^+, Mg^{2+}, Al^{3+}, Si^{4+}), $\lambda_i < 125$ nm accounting for their transparency and low dispersion and index. Oxides and silicates containing open-shell (transition metal) ions have $\lambda_i > 125$ nm, and their compounds are often coloured, displaying high dispersion and index. The optical properties of materials containing both closed- and open-shell ions are often determined by the latter, as a comparison of (say) jadeite with acmite or clinozoisite with epidote will show.

Wavelength-dependence (dispersion) of indices. Having related the refractive index to the absorption spectrum, it is instructive to consider an example. Because of the experimental difficulties, few reliable spectra have been published of minerals having strong absorption in the near ultra-violet, and we therefore use data for dilute aqueous solutions of Fe^{3+}. Fig. 1 shows that this ion has three strong absorption bands between 200 and 400 nm, and there will be further absorptions in the vacuum ultra-violet ($\lambda < 185$ nm). We use a four-band model to represent the properties of a hypothetical material containing Fe^{3+} coordinated by oxygen. The first three bands have the properties (λ_i, I_i) of the three bands in fig. 1 and the fourth band takes the place of the absorptions in the vacuum ultra-violet. Values of I_i have been scaled
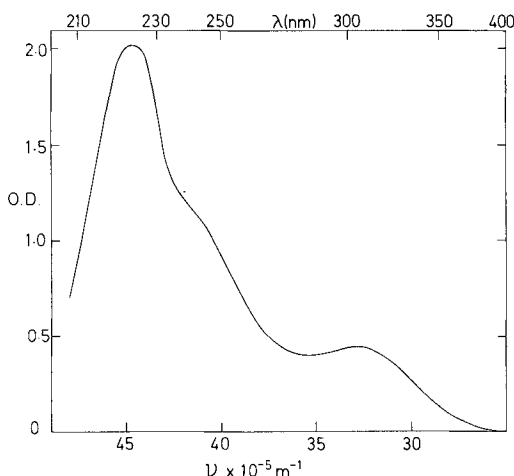
FIG. 1. The near-ultra-violet absorption spectrum of Fe^{3+} in aqueous solution. Curve resolution reveals three bands at 307·7, about 250, and 223·7 nm. Cell thickness 1 cm $[Fe^{3+}] = 2 \times 10^{-4}M$ in $1M$ H_2SO_4.

to a concentration of 1 Fe^{3+} in 100 Å³, assuming Beer's law holds. Inspection of Table I will show the following interesting features. The refractive index and dispersion are comparable with those of Fe^{3+}-rich minerals such as andradite, acmite, goethite, and epidote. About three-fifths of the dispersion is caused by the three near-ultra-violet bands, with the largest single contribution coming from the relatively weak band at 307·7 nm, for which the large variation in L more than compensates for the low value of I. One-eighth of the contribution to $(\bar{n} - 1)$ comes from the three near-ultra-violet bands. This model illustrates the way in which the optical properties of an ionic material in the visible

region are determined mainly by the wavelengths and integrated absorbances of bands in the near ultra-violet, many of which involve ligand–metal charge-transfer processes, e.g. $(Fe^{2+}, O^{2-}) \xrightarrow{h\nu} (Fe^{+}, O^{-})$, $(Fe^{3+}, O^{2-}) \xrightarrow{h\nu} (Fe^{2+}, O^{-})$. These bands typically move towards the visible (thus increasing index and dispersion) with increasing formal charge on the metal ion, with increasing covalency, and with decreasing metal–oxygen distance. They are always polarized along the oxygen–metal vector (Smith and Strens, 1976), and their wavelengths vary with direction in distorted coordination polyhedra, thus contributing to the optical anisotropy of such phases as acmite, epidote, and viridine.

Composition dependence of indices and extinction angles. The composition dependence of optical properties results from the appearance of new absorption bands and the disappearance of bands previously present as the composition changes. The simplest case is that of an isotropic binary solid solution obeying Beer's and Vegard's laws, in which the index at some chosen wavelength is given by:

$$n^2(\lambda) = 1 + xa + (1 - x)b \qquad (7)$$

where $0 \leqslant x \leqslant 1$ is the compositional variable, and a, b, are the values of $n^2 - 1 = IL/\pi^2$ at $x = 0$ and $x = 1$ respectively. In anisotropic crystals, (7) applies to the unique (b) direction of a monoclinic crystal, and to each of the two (or three) principal indices of uniaxial and orthorhombic biaxial crystals. For the (010) plane of monoclinic crystals, a more complex equation is required to allow for the continuous change in the absorption spectrum that occurs as the indicatrix rotates about b with changing composition or wavelength. The simplest equation appears to be of the form:

TABLE I. *Properties of a hypothetical isotropic Fe^{3+} compound having the spectrum shown in fig. 1*

i	λ_i (nm)	I_i	L_F	L_D	L_C	IL_F	IL_D	IL_C	Dispersion F–C
1	307·7	0·5835	1·6686	1·3748	1·2817	0·9736	0·8022	0·7479	0·2257
2	250·0	0·6052	1·3596	1·2195	1·1697	0·8228	0·7380	0·7079	0·1149
3	223·7	1·3016	1·2687	1·1684	1·1315	1·6513	1·5207	1·4737	0·1776
4	100·0	16·4000	1·0442	1·0297	1·0238	17·1247	16·8863	16·7898	0·3349
					ΣIL	20·5725	19·9472	19·7193	0·8531
		index with bands 1–4			n	1·7563	1·7381	1·7315	0·0248
		index with band 4 only			n	1·6538	1·6465	1·1435	0·0103
		effect of bands 1–3			Δn	0·1024	0·0916	0·0879	0·0145

The integrated intensities (I_i) are normalized to a concentration of 1 Fe^{3+} ion in 100 Å³ (similar to that in acmite) assuming a Gaussian form-factor. Band 4 represents the effects of all absorption bands in the vacuum ultra-violet (below 185 nm), and its wavelength and integrated intensity are assumed to remain constant as iron enters the structure. If Fe^{3+} replaces Al, then both ΣI_i and λ_i will increase because of the larger number of electrons and the lower ionization potential of Fe^{3+} (note that $\Sigma f_i = Z$, the number of electrons in the system). This will make the effect of Fe^{3+} larger than that calculated above.

$$n^{2'} = 1 + (1-x)((\mathbf{a}_1 \cos^2\varphi' + \mathbf{a}_2 \sin^2\varphi') +$$
$$+ x(\mathbf{b}_1 \cos^2(\varphi' - \theta) + \mathbf{b}_2 \sin^2(\varphi' - \theta)). \quad (8)$$

Here, $\mathbf{a}_1$, $\mathbf{a}_2$ and $\mathbf{b}_1$, $\mathbf{b}_2$ are vectors, being the values of $(n^2 - 1) = IL/\pi^2$ for the two principal indices in the (010) section at $x = 0$ and $x = 1$; θ is the angle (or, where appropriate, its complement) through which the indicatrix rotates between $x = 0$ and $x = 1$, and φ' is the angle between $\mathbf{a}_1$ and the vibration direction being considered. Primed quantities (n', φ') refer to general directions, others (n, φ) to the principal indices; thus φ is an extinction angle, φ' is not. The (n, φ) may be determined by finding the maximum and minimum values of $n^{2'}$. In addition to the assumptions implicit in (7), it is assumed that the transition moments of the oscillators (which determine I) remain fixed in orientation as the composition changes. The angular dependence arises because the projections of the transition moments on the indicatrix axes vary as $\cos \varphi$ or $\sin \varphi$, and the I_i are proportional to the squares of the transition moments. Fig. 2 compares observed and calculated variations of index and extinction angle in the monoclinic Al–Fe epidote solid solution series in which a large (95°) rotation of the indicatrix occurs. Considering the number and nature of the assumptions used, the agreement is satisfactory.

Volume dependence of the mean index. The dependence of the mean index $\bar{n} = (\omega^2\epsilon)^{\frac{1}{3}}$ or $\bar{n} = (\alpha\beta\gamma)^{\frac{1}{3}}$ on volume may also be deduced from the Helmholtz or Sellmeier equations if it is assumed that I is proportional to N/V, i.e. that Beer's law is obeyed. At constant (N, λ, λ_i), (6b) then leads to the Newton–Laplace relation $V(n^2 - 1) = \text{constant}$. This is important, because it enables changes in index caused by the same substitution occurring in different minerals to be corrected for differences in dilution, placing them on a comparable basis. For example, fayalite contains 8 Fe^{2+} ions in a unit cell of volume 307 $Å^3$, whereas the iron cordierite sekaninaite has the same number in a volume of 1507 $Å^3$. The increase in mean index caused by complete replacement of Mg by Fe^{2+} differs by a factor of five, being 0·041 in cordierite and 0·209 in olivine. When allowance is made for the difference in volume, the changes in refractivity are identical within experimental error, as would be expected from the similar (Mg, Fe) site geometries.

Discussion. The modified Sellmeier equation (6b) may be used to derive the wavelength-, volume-, and composition-dependence of the refractive indices and extinction angles of transparent mixcrystals. It is clearly possible to generalize (8) to triclinic crystals and solid solutions with many components, and to allow for deviations from Vegard's and Beer's laws. To the extent that the
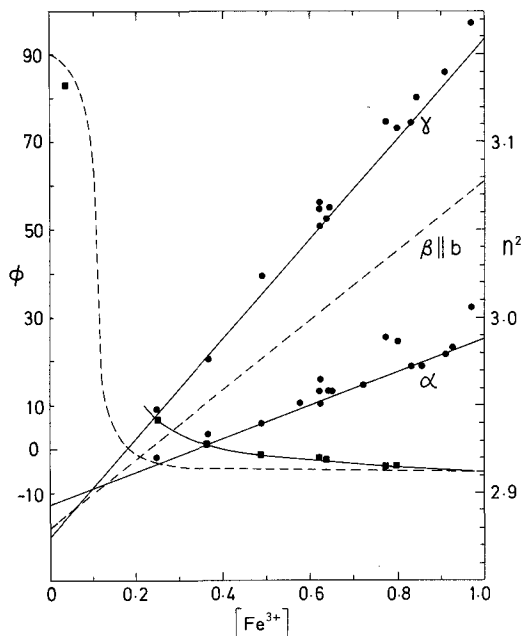

FIG. 2. Comparison of observed α and γ indices (●) and extinction angles (■) of (Al, Fe) epidotes with those calculated using equation (8), taking values of $\mathbf{a}_1 = 1\cdot8744$, $\mathbf{a}_2 = 1\cdot8934$, $\mathbf{b}_1 = 2\cdot1854$, $\mathbf{b}_2 = 1\cdot9887$, $\theta = 5°$ appropriate to Fe^{3+} entering the $M(3)$ position. Data are from Myer (1966) and Deer, Howie, and Zussman (1962, 1, table 33). The calculations show iron-poor epidotes becoming uniaxial three times within a narrow range of compositions. At $[Fe^{3+}] \simeq 0\cdot06$ and $0\cdot13$, ϵ lies in the (010) plane, and at $[Fe^{3+}] \simeq 0\cdot10$, ϵ is normal to (010). This behaviour accounts for the anomalous interference colours, rapid variation of $2V$ and extinction angle in zoned crystals, occasional crossed dispersion, and very rapid changes in φ and $2V$ with wavelength seen in many clinozoisites (Johnston, 1949; Deer, Howie, and Zussman, 1962, 1, figs. 48 and 49). The extinction angle is undefined at $[Fe^{3+}] \simeq 0\cdot1$, where $d\varphi/dx \to \infty$, but this composition will vary with wavelength, minor element content, and conditions of formation. The squares of the principal indices vary linearly with composition, despite the 95° rotation of the indicatrix. As $\Delta n/n \ll 1$, the individual indices also approximate linear variation with composition. With increasing iron content, the indices show increasing positive deviations from the trend for iron entering the $M(3)$ position, as more iron enters $M(1)$, for which position $\mathbf{b}_1$ and $\mathbf{b}_2$ are substantially higher.

spectra may be related to the structure, the structure-dependence of properties may also be found.

Thus far, the substituents have been assumed not to interact, i.e. the (f_i, λ_i) do not vary with composition or volume. In general this will not be true, although interactions appear to be negligible for most closed-shell ions, for open-shell (transition

metal) ions of formal charge $\leqslant 2$ in linked poly-
hedra, and for open-shell ions of higher formal
charge in isolated polyhedra.

Strongly coloured materials

Strong colours may be caused by absorption in
the visible region by the long wavelength tails of
bands in the near ultra-violet (e.g. hematite), by the
short wavelength heads of bands in the near infra-
red (e.g. the 725 nm band responsible for the
pleochroism of chlorite), or by bands in the visible
region itself, e.g. that at 550 nm in the γ spectrum
of piemontite, which makes the mineral nearly
opaque in thin section (Burns and Strens, 1967).
How does this strong absorption affect the optical
properties?

For media with a strong band in the visible
region, the index is most easily calculated using
a combination of Sellmeier (for bands with
$(\lambda - \lambda_i)$ $w_i \gg 1$) and Helmholtz equations:

$$n^2 = 1 + k^2 + S + H \qquad (9)$$

where $S = IL/\pi^2$, and H is the contribution of the
strong band in the visible, evaluated using equation
(5a). Fig. 3 shows that the dispersion curve of
piemontite should have a marked anomaly near
550 nm, with changes in index of ± 0.002 extending
well beyond the visible region. In a crystal with
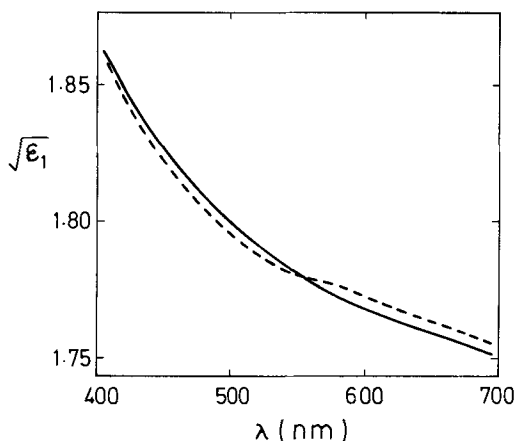small birefringences, extreme dispersion of both 2V

FIG. 3. Dispersion of $\sqrt{\{\varepsilon_1(\gamma)\}} \simeq \gamma$ of a piemontite with
one Mn^{3+} ion per formula unit in the $M(3)$ position
calculated using the Sellmeier equation (6b) with $I_i = 20$,
$\lambda_i = 170$ nm (solid line), and using equation (9) with
$\lambda_i = 550$ nm, $w_i = 110$ nm, $a_i = 3 \cdot 10^5 m^{-1}$ (dashed line).
The strong band at 550 nm in the γ spectrum (Burns
and Strens, 1967) significantly affects the index through-
out the visible region, the anomaly approaching $+0.007$
at 575 nm, and -0.006 at 525 nm.

and extinction angle may occur near bands with
$a_i > 10^5 m^{-1}$.

If the medium is coloured by a band outside the
visible region, the dispersion may be high (as in
hematite), but it will not appear anomalous, and the
Sellmeier equation remains a good approximation
up to values of the linear absorption coefficient at
which k^2 and ε_2 are no longer negligible compared
with n^2 and ε_1. For piemontite, $a_i \simeq 3 \cdot 10^5 m^{-1}$,
$\lambda_i = 550$ nm, $k = 0.013$, and if $n = 1.8$, $k^2/n^2 =$
$5 \cdot 10^{-5}$ which is negligible, but $\varepsilon_2/\varepsilon_1 = 0.014$,
which is becoming significant. In practice, the
Sellmeier equation may be applied to media that
transmit sufficient light to be studied in normal
(30 μm) thin sections, but the Helmholtz equa-
tions should be applied to those that are best ex-
amined using polished surfaces and reflected light.

Optics of opaque media

The optical properties of an opaque medium are
completely specified by any one of the quantities n,
$k, \varepsilon_1, \varepsilon_2$ given over the whole spectrum ($0 < \lambda < \infty$).
In practice, two such quantities (usually n and k, or
ε_1 and ε_2) are specified at one or more wavelengths.
As these properties can seldom be measured
directly, they are usually obtained indirectly from
reflectance measurements. The specular reflectance
(R) at normal incidence is given by Fresnel's
equation, written in the form:

$$R = \frac{(N - \mu)^2}{(N + \mu)^2} = \frac{(n - \mu)^2 + k^2}{(n + \mu)^2 + k^2} \qquad (10)$$

where $N = n - ik'$ is the complex refractive index of
the opaque material in contact with a transparent
isotropic medium (air or immersion oil) of index μ,
and $k' = k/n$. Note that $N^2 = (n - ik')(n + ik')$. In
air, $\mu \simeq 1$, and if $k = 0$, (10) becomes the fami-
liar expression for the reflectance of a dielectric:
$R = (n - 1)^2/(n + 1)^2$. The complex refractive index
is defined in terms of the complex dielectric func-
tion ε by:

$$N^2 = \varepsilon = \varepsilon_1 + i\varepsilon_2, \quad \varepsilon_1 = n^2 - k^2, \quad \varepsilon_2 = 2nk.$$

As ε_1 and ε_2 are the solutions of the Helmholtz
equations (5a, 5b), it is possible to relate the optical
properties of opaque media to their spectra using
methods analogous to those already applied to
transparent and coloured media. For this purpose,
it is convenient to represent the properties in the ε_1,
ε_2 plane, rather than to plot $R, n, k, \varepsilon_1, \varepsilon_2$ against
wavelength. The Helmholtz equations may then be
used to find how the observed properties (R, n, k)
will be affected by changes in the position, width, or
absorbance of bands in the spectrum. Conversion
of $(\varepsilon_1, \varepsilon_2)$ to (R, n, k) is conveniently achieved using
charts contoured in R or n and k, such as those in
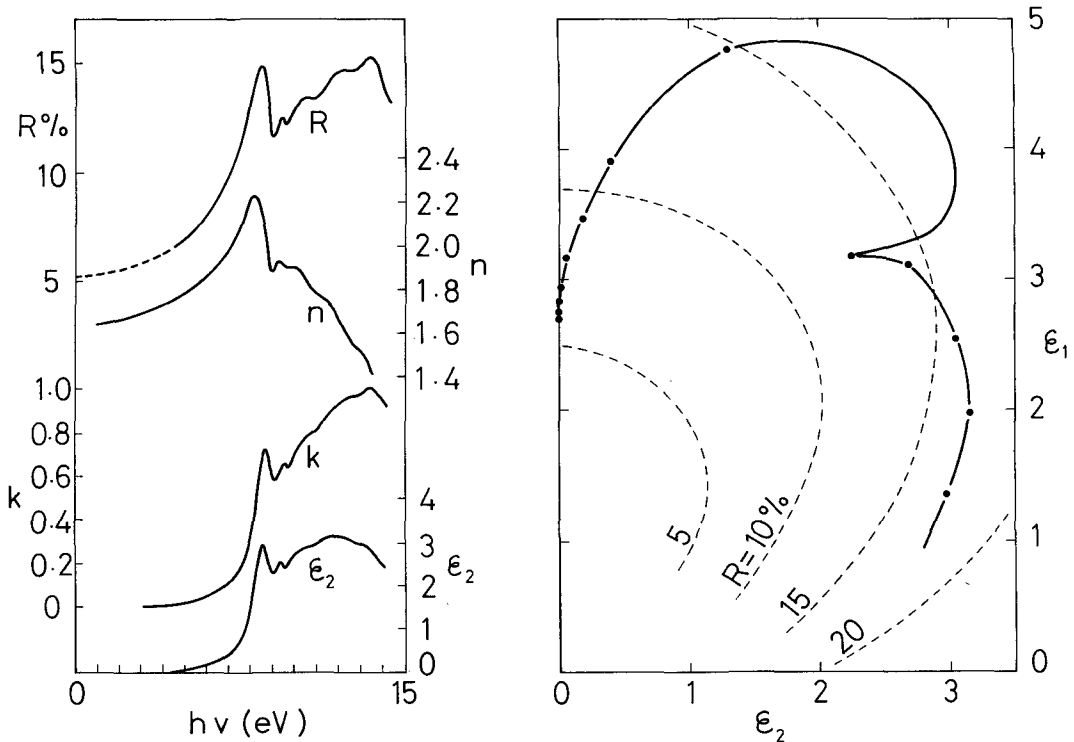figs. $4b$ and $5b$.

FIG. 4a and 4b. The optical properties of synthetic forsterite determined by Nitsan and Shankland (1976) for photon energies between about 4 and 14 eV. To an observer with eyes sensitive over this range, forsterite would appear transparent in thin (30 μm) section well into the ultra-violet, becoming strongly coloured at about 300 nm, and opaque at shorter wavelengths. Similarly, materials that are opaque in the visible region usually transmit light in the infra-red, e.g. Wood's (1971) work shows that stibnite (Sb_2S_3) is transparent at photon energies below about 1·3 eV (950 nm). a (*left*). Observed specular reflectance (R) of synthetic forsterite measured using unpolarized light falling at near-normal (82°) incidence on a polished (010) surface, together with values of n, k, and ε_2 obtained by Kramers-Kronig analysis of the reflectance data. The true reflectance is about 1·13 times the observed value, due to the effects of surface imperfections (with $k = 0.7$, $\lambda = 140$ nm, $a = 6 \times 10^7$ m^{-1}, most of the incident light is absorbed or reflected within $\lambda/10$ of the surface: the measurements are therefore very sensitive to surface quality). Note the well-defined exciton band at 8·72 eV in the ε_2 spectrum. The band gap is $(8·72 + E)$ eV, where E is the binding energy of the exciton, estimated by Nitsan and Shankland (1976) as about 0·1 eV. The band width (w) is twice the difference between the energies of the maxima in the n (8·16 eV) and ε_2 (8·72 eV) spectra, or about 1·1 eV. The maximum in the reflectance spectrum (8·58 eV) does not coincide with the centre of the exciton band, which is defined by the maximum in ε_2. The fine structure of the R, k, and ε_2 (but not n) spectra is qualitatively similar if these small energy differences are ignored, and reflectance spectra thus provide a good indication of the positions and relative intensities of the absorption bands. b (*right*). The optical properties of forsterite represented in the ε_1-ε_2 plane, with reflectance contours superimposed. The markers (●) are at intervals of 1 eV from 1 to 13 eV, and their spacing is a measure of dispersion. Note the transparent region ($\varepsilon_2 = 0$) at low photon energies, and the increasing dispersion as the exciton band is approached. The Helmholtz equations may be used to calculate the displacement of any point on the curve (and, using the reflectance contours, the changes in reflectance) that would be caused by a given change in band energy, width, or absorbance.

Figs. 4 and 5 show the optical properties of forsterite (Mg_2SiO_4) and covelline (CuS) plotted conventionally and in the (ε_1, ε_2) plane. Forsterite is transparent in the visible region, but in common with all other materials it is opaque at energies above the band gap, which marks the first strong transition between the valence and conduction bands (Kittel, 1966). The band gap in covelline lies in the infra-red, and this mineral is opaque in the visible region.

Inspection of the Helmholtz equations (5a, 5b) and of figs. 4 and 5 will show that the proximity of absorption bands makes the optical properties of opaque media much more sensitive to small variations in band parameters (a_i, λ_i, w_i) than those of transparent media, and that quite minor changes in
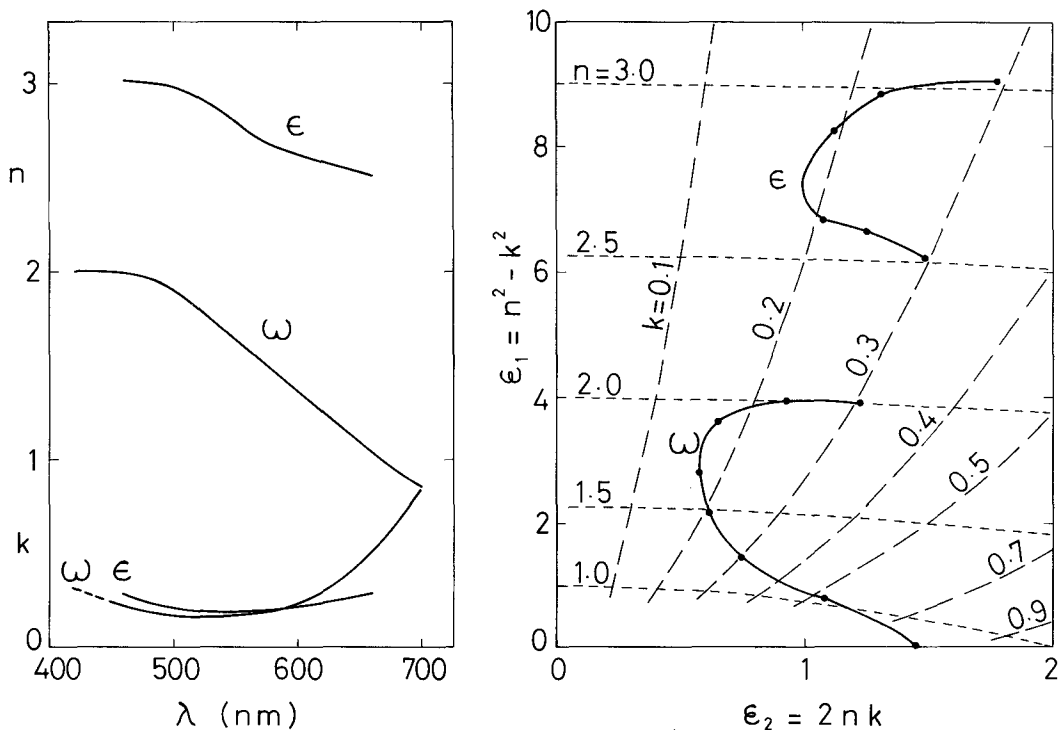
FIG. 5a and 5b. The optical properties of a natural covelline (CuS) determined by Gehlen and Piller (1965) by measurement of reflectance at perpendicular incidence in air and in oil. Diffuse reflectance spectra measured by Wood (1971) suggest a band gap of about 1·2 eV, implying that covelline should be transparent at infra-red wavelengths longer than about 1 μm. a (left), values of n and k for the ω and ε vibration directions computed from reflectance data by Gehlen and Piller (1965). The upper part of the figure shows the dispersion of ε (460–660 nm) and ω (420–700 nm) indices, and the lower part the dispersion of k, which has a minimum in both polarizations between 500 and 600 nm, indicating the presence of strong absorption bands in both the near ultra-violet and the near infra-red. The marked anisotropy of n and k leads to strong bireflection, and the dispersion of n in particular causes reflectances in air to be higher for blue light, giving the mineral its characteristic colour. b (right), the optical properties of covelline represented in the ε_1–ε_2 plane, with contours of n and k superimposed. For the ε spectrum the markers (●) are at intervals of 40 nm from 460 to 660 nm. For the ω spectrum, the markers are at 40 nm intervals from 420 to 700 nm (where ε_1 is about to become negative). The strong anisotropy of covelline is demonstrated by the complete separation of the ω and ε curves. The Helmholtz equations may be used to calculate the displacement of any point on the curves (and, using the n and k contours, the changes in those quantities) that would be caused by given changes in band energies, widths, or absorbances. Changes in reflectance may also be found (see fig. 4b).

composition or crystal structure may cause major variations in (R, n, k).

The wavelength (λ_i) at which absorption occurs depends mainly upon interatomic distance, and it will therefore be affected by pressure, temperature, composition, and crystal structure. The absorbance (a_i) depends mainly on concentration (N_i/V). The band width (w_i) increases with the absolute temperature and with the concentration of the chromophore, and it may be expected to vary inversely as some power of the interatomic distance: the width is commonly one-tenth to one-third of the transition energy. The band shape is also important: it is approximately Gaussian for most d-d bands (which are thermally broadened), but the stronger interband transitions such as the O → Fe^{3+} charge-transfer band at 223·7 nm in fig. 1, and the exciton band at 8·8 eV in fig. 4a, approach Lorentzian shape.

The optical properties of opaque media should thus show marked dependence on structure, composition, temperature, and pressure, but detailed correlations can only be made when optical data are available for all bands that contribute significantly to the properties at the wavelength considered, i.e. measurements must extend over a range large compared with the widths of the nearby absorption bands. Reliable optical data for opaque minerals are seldom available beyond the visible region, and they are often confined to a

few discrete wavelengths in the visible. Excellent spectra are available for many semiconductors of technological importance but these are usually very simple in chemistry and crystal structure.

Wood and Strens (1970) and Wood (1971) have determined the diffuse reflectance spectra of many important opaque oxide and chalcogenide minerals over the range 0·5 to 6·0 eV, and these spectra provide some indication of the positions of the band gaps and of the main absorption bands, but values of (R, n, k) cannot be extracted from diffuse reflectance spectra, and information on the anisotropy is lost.

Optical anisotropy

Birefringence in weak absorbers and bireflectance in opaque phases are both caused by the direction-dependence of absorption, i.e. by pleochroism. The birefringence of weak absorbers in the visible region depends mainly on pleochroism in the ultra-violet, but the bireflectance of opaque phases depends also on the pleochroism of bands in the visible and near infra-red. The structural origins of pleochroism and of optical anisotropy are thus linked, and use of the modified Helmholtz (5a, 5b) and Sellmeier (6b) equations provides an alternative to Bragg's (1924) approach to the calculation of optical anisotropy from structure data when the structure-dependence of the spectra is known. The necessary spectral data are slowly becoming available for the important transparent and strongly coloured phases, but for opaque phases they are still inadequate both in quality and quantity.

We distinguish three cases: first, Bragg's methods as developed by Fawcett (1963a) may be applied quantitatively to many weakly absorbing phases of simple chemistry and structure, e.g. calcite ($CaCO_3$) and rutile (TiO_2). The calculation involves lattice sums, and requires a computer. The Sellmeier equation may also be used if the necessary spectroscopic data are available, and this requires only a four-function calculator. Secondly, for weakly absorbing phases of more complex chemistry and structure (including most minerals studied in thin section), the Bragg method can provide only qualitative results, and the Sellmeier or Helmholtz equations are used. Finally, for opaque phases, the problem is approached using the modified Helmholtz equations (5a, 5b), the calculations being within the capacity of a simple programmable calculator.

Simple transparent phases. When isotropic ions aggregate, they distort (polarize) the electron shells of their neighbours and are themselves polarized by those neighbours. If the crystal is of less than cubic symmetry, then optical anisotropy will develop. The strength of this anisotropy depends mainly

upon the geometry of the structure, the polarizabilities of the ions, and the interionic distances. For the simple case of two ions of equal and initially isotropic polarizability α separated by a distance r long compared with the sum of their radii, and with the electric vector first parallel and then perpendicular to the interionic vector, the polarizabilities become:

$$\alpha'_\parallel = \frac{\alpha}{1 - (2\alpha/r^3)}, \qquad \alpha'_\perp = \frac{\alpha}{1 + (\alpha/r^3)} \qquad (11)$$

so that even a simple diatomic molecule is optically anisotropic.

The extreme birefringence of many carbonates and nitrates, discussed by Bragg (1924) and by Hartshorne and Stuart (1960), arises because triangular CO_3 and NO_3 complex anions have small polarizabilities along their triad axes, and large polarizabilities in the plane containing the three short O–O vectors. When such strongly anisotropic complex anions are stacked with their triad axes parallel, the crystal is strongly birefringent, e.g. in calcite $\omega = 1\cdot6583$, $\epsilon = 1\cdot4863$, $(\omega - \epsilon)/(\epsilon - 1) = 0\cdot35$. When the same complex anions are disposed with cubic symmetry, as in $Pb(NO_3)_2$, the crystal remains isotropic.

The link between polarizability and refractive index is provided by the Lorenz–Lorentz equation, which may be written:

$$M = V\left(\frac{n^2 - 1}{n^2 + 2}\right) = \frac{4\pi}{3}\sum n_j \alpha_j, \qquad (12)$$

where M is the molar refractivity, and the N_j, α_j are the number and polarizability of the jth type of ion, atom, or molecule. If $M/V = \eta$, then the mean index may be recovered by:

$$\bar{n} = [(1 + 2\eta)/(1 - \eta)]^{\frac{1}{2}}. \qquad (13)$$

When only one type of atom or molecule is present ($q = 1$), the polarizability is related to the (I_i, λ_i) by:

$$\alpha_j = \frac{1}{4\pi^2} \frac{V}{N_j} \sum \frac{I_i \lambda^2}{\lambda^2 - \lambda_i^2}. \qquad (14)$$

Substitution of (14) into (12) then gives (15), which may be compared with (6b):

$$\frac{n^2 - 1}{n^2 + 2} = \frac{1}{3\pi} \sum \frac{I_i \lambda^2}{\lambda^2 - \lambda_i^2}. \qquad (15)$$

When $q \geqslant 2$, it is in general no longer possible to calculate polarizabilities from the spectra. For example, in a medium containing Fe^{3+} and O^{2-}, the $O \rightarrow Fe^{3+}$ charge-transfer bands (fig. 1) contribute strongly to (15), but their effect cannot be assigned to any one atom or be divided between atoms in any but an arbitrary way. This means that equations (12) and (15) cannot be used as the basis of a calculation of anisotropy when $q \geqslant 2$.
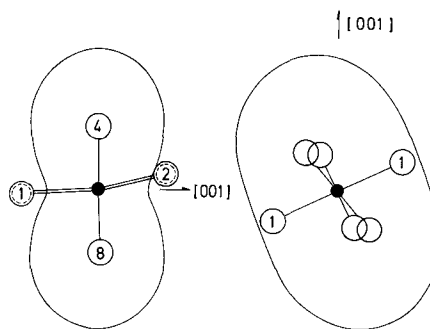
No such restriction applies to the Sellmeier and Helmholtz equations, which do not require the assumption that a particular absorption band belongs to a particular atom, ion, or molecule.

Bragg's method relies on the use of the Lorenz–Lorentz equation, and in its original form suffered from two serious defects. It involved a slowly converging lattice sum that was difficult to evaluate before the arrival of computers, and it assumed initially isotropic polarizabilities for Ca^{2+} and O^{2-} (carbon was assumed to have negligible polarizability). These problems were tackled by Fawcett (1963a, b) and by Bolton, Fawcett, and Gurney (1962), who applied similar methods to rutile, anatase, and brookite. These authors improved the convergence of the lattice sum by summing over an element having the shape of the unit cell, and they also allowed for the anisotropic polarizability of the oxygen ions, assuming Ti^{4+} to have a small isotropic polarizability of 0.2 $Å^3$. Each oxygen ion in rutile is bonded to three coplanar titanium ions, so that the electron cloud of the polarizable oxygens is drawn out in the (110) plane, resulting in a polarizability of 1.73 $Å^3$ for $E \perp (110)$ and 2.58 $Å^3$ for E in (110). This is a substantial advance on Bragg's method and assumptions, but the method is still limited to chemically and structurally simple phases by the need to apply $p(q-1)$ constraints to force a solution, where p is the number of non-zero elements in the polarizability tensor of the crystal, and q is the number of inequivalent atoms in the unit cell.

Complex transparent phases. In compounds containing only closed-shell ions of neon or argon configuration (O^{2-}, F^-, Na^+, Mg^{2+}, Al^{3+}, Si^{4+}, K^+, Ca^{2+}), the anion polarizabilities are large compared with those of the cations, and this, combined with the effect of the α/r^3 terms of equation (11) causes the optical anisotropy of these compounds to be dominated by a few short anion-anion vectors. The optical orientations of many chain and sheet silicates may be rationalized if it is assumed that there is a concentration of O–O vectors near the chain axis or in the plane of the sheet. Thus, γ often lies near the chain axis (c) in pyroxenes and amphiboles, and α is nearly normal to the sheet in most sheet silicates, with $\beta \simeq \gamma$ in the plane of the sheet. In aluminosilicates, the shortest O–O vectors are often those of the shared edges of $[AlO_6]$ octahedra forming the chain. These shared edges are normal to the chain axis, and andalusite, sillimanite, zoisite, and iron-poor clinozoisite all have γ normal to the chain. Although these applications of the ideas advanced by Bragg (1924), Wooster (1931), and Hartshorne and Stuart (1960) are qualitative, they are none the less useful.

When open-shell (transition metal) ions, especially those of formal charge $\geqslant 3$, enter the structure, the optics become much more confused. The general rule is that the anisotropy becomes more closely related to the distortions of the coordination polyhedra about the transition metal ion (Strens, 1967). Examples include the andalusite-viridine, jadeite-acmite, and clinozoisite-epidote solid-solution series. The explanation is that the near-ultra-violet O → M charge-transfer bands (fig. 1) are polarized along the metal–oxygen vectors, and their λ_i increase with decreasing metal–oxygen distance: their contributions to the index are therefore greatest for vibration directions near the short M–O bonds,

$\uparrow$[001]

[001]

FIG. 6a and 6b: 6a (*left*). Structure dependence of the principal indices in the optic axial plane (010) of Al–Fe–Mn epidotes (fig. 2 and Strens, 1967). The hourglass shape represents the change in index as a function of direction caused by complete replacement of Al in the M(3) position by Mn^{3+}. The effect of Fe^{3+} is very similar. The increase in index is greatest for the vibration direction near the short $O(4)$–Mn^{3+}–$O(8)$ bonds (1.90, 1.86 Å), and least for directions near the long $O(1)$–Mn^{3+}–$O(2)$ bonds (2.27, 2.03 Å). As a result, the indicatrix rotates very rapidly about $[010] = \beta$ (see fig. 2) and the birefringence increases from about 0.006 to 0.048 as Mn^{3+} or Fe^{3+} fills the M(3) position. This behaviour is to be expected if the O → Mn^{3+} charge-transfer bands in the near ultra-violet move towards the visible region with decreasing metal-oxygen distance in the manner shown by the first near-ultra-violet band in synthetic piemontite (Langer et al., 1976). Since the absorption by Al lies in the vacuum ultra-violet (below 100 nm), its removal has little effect on either mean index or anisotropy. 6b (*right*). Structure dependence of the principal indices in the optic axial plane (010) of minerals in the jadeite-acmite solid solution series. The centrosymmetric oval represents the change in index as a function of direction caused by complete replacement of Al in the M(1) position by Fe^{3+} (Freer, 1973). The increase in index is least for vibration directions near the long (2.11 Å) Fe^{3+}–O(1) bonds, and greatest for directions near the short (1.94, 2.03 Å) bonds. The result is that birefringence increases with iron content from about 0.012 in jadeite to 0.060 in acmite, and the indicatrix rotates about $b = \beta$ from γ:[001] $\simeq 38°$ (jadeite) to γ:[001] $= 99°$ (acmite).

TABLE II. *Parameters of the near-ultra-violet* $O \to Mn^{3+}$ *charge-transfer bands in synthetic piemontite. Sample thickness assumed to be 12 μm. I is the integrated absorbance normalized to 1·0 Mn^{3+} per formula unit. L is $\lambda^2/(\lambda^2 - \lambda_i^2)$. w_i is the full width at half maximum absorbance. λ_i is not the wavelength of maximum absorbance, but that found by taking moments. Source of spectra is Langer et al. (1976) fig. 1*

	λ_i (nm)	w_i (nm)	L	$10^3 I$	$10^3 IL$
$\alpha'[001]$	283·7	53·1	1·3017	56·2	73·2
$\beta[010]$	261·4	63·5	1·2540	70·2	87·4
γ'	270·3	82·8	1·2664	97·6	123·6

TABLE III. *Effect on the optical properties of clinozoisite at 589·3 nm of bands having the properties given in Table II calculated using equation (6b)*

	$\alpha'[001]$	$\beta[010]$	γ'
$(n_D^2 - 1)$ clinozoisite	1·8934	1·8805	1·8744
IL from Table II(a)*	0·0073	0·0087	0·0124
calc. change in n_D*	0·0022	0·0025	0·0037
obs. change in n_D*	0·0322	0·0543	0·0860

* For complete replacement of Al in $M(3)$ by Mn^{3+} (Freer, 1973).

and least for directions near the long bonds (fig. 6a, b). There is other good evidence for dependence of the λ_i on M–O distance, a particularly interesting example being the spectrum of synthetic piemontite described by Langer et al. (1976). This shows the first strong $O \to Mn^{3+}$ charge-transfer band at 261 to 284 nm in all three polarizations. The bands are strongly pleochroic, with $\lambda_i = 284, 261$, and 270 nm and $1000I_i = 56, 70$, and 98 in α, β, and γ spectra respectively (Table II). Their contributions to the IL term of equation (6b) are strongly anisotropic, but they explain only a small proportion of the observed changes in index (Table III), bands beyond 200 nm presumably accounting for the rest. Substitution of Fe^{3+} into the epidote $M(3)$ position has a similar effect on the optics to that of Mn^{3+}, and pleochroism of the near-ultra-violet $O \to Fe^{3+}$ charge-transfer bands is predicted to occur in the Al–Fe epidotes. The corresponding charge-transfer bands in minerals containing bivalent ions (Fe^{2+}, Mn^{2+}, etc.) lie further into the ultra-violet, and the correlation between site distortion and optics is much less marked.

A particularly striking example of the structure-dependence of optics is provided by sphene ($CaTiSiO_5$), in which the γ index coincides with the axis of a chain formed by corner-sharing [TiO_6] octahedra. The average Ti–O distances parallel and normal to the chain axis are 1·87 and 2·00 Å respectively.

Opaque phases. The problem of relating optical anisotropy (bireflectance) in opaque phases to the structure is essentially that of determining how the energies, and to a smaller extent the intensities and widths, of absorption bands depend on interatomic distance and other structural variables. More and better spectroscopic data are urgently needed, but some useful work can be done using published k values to estimate the magnitude of the a_i, and diffuse reflectance spectra (Wood, 1971) to establish

approximate band widths, positions, and relative intensities. Use of equations (5a, 5b) and charts relating $\varepsilon_1, \varepsilon_2$ to (R, n, k) then allows one to investigate the likely causes of anisotropy.

Discussion and conclusions

The mineralogical literature contains abundant descriptions of optical properties, but remarkably few discussions of the reasons why particular minerals display particular properties. The origins of the optical properties of the commonest non-opaque minerals are seldom understood even qualitatively, and few quantitative studies have been attempted. There can be few fields of scientific endeavour in which so little progress has been made in the last century, or in which so many workers make and use observations of properties without knowledge or understanding of their origin. With the increasing availability of spectral and structure data, and the development of methods of calculating the effect of changes in structure on spectra (e.g. Wood and Strens, 1972; Tossell et al., 1974), a quantitative rather than a descriptive approach to mineral optics has become possible.

One of the simplest tools used by the mineralogist is the optical variation diagram, which expresses the relationship between composition and indicatrix orientation (extinction angle) and shape (principal indices). Many assumptions are implicit in the use of such diagrams, which do not in general provide a satisfactory representation of the optical properties of structurally and chemically complex crystals. For example, many diagrams show scatter or curvature because differences in cation distribution lead to different optical properties for crystals of identical bulk composition (see Deer, Howie, and Zussman, **2**, 257, 296, 298; **4**, 130 and 131). Only when compositional variables are properly defined (using site populations rather than bulk compositions when necessary), and variations in concentration per unit volume are considered, does it become possible to determine the true dependence of refractivity on composition, to detect

deviations from linearity caused by the interaction of substituents, and to test the equations of crystal optics against the experimental data.

The wavelength-dependence (dispersion) and volume-dependence of optical properties are rather more easily described, at least for transparent minerals in the visible region, and for small variations in volume. However, there are no less than three equations that may be used to calculate the volume-dependence of indices (Lorenz–Lorentz, Newton–Laplace, and Gladstone–Dale), and these will be compared in a later paper.

The quantitative treatment of optical anisotropy still presents problems, but as our knowledge and understanding of mineral spectra expands, the origins of anisotropy will become increasingly clear. The urgent need is for measurements of the ultra-violet spectra of transparent minerals, with particular emphasis on establishing the dependence of absorption band parameters (a_i, λ_i, w_i) upon interatomic distance and other structural variables. Among the opaque minerals, the need is for more accurate data spanning a wider range of wavelengths (say from 200 to 2000 nm) rather than measurements restricted to the visible region (400 to 700 nm). Because of the proximity of strong absorption bands, the optics of opaque minerals will show extreme sensitivity to changes in wavelength and composition, and it may ultimately prove easier to account for the anisotropy of opaque than of transparent phases.

It is often useful to represent the optical properties of opaque materials in the ε_1–ε_2 plane rather than as plots of n, k, R against wavelength or photon energy. Apart from the ease with which ε_1 and ε_2 may be calculated from the spectra using the Helmholtz equations, values of (R, n, k) may be found (figs. $4b$, $5b$).

The second and third papers in this series will apply the classical theory to the optical properties of common transparent and opaque minerals.

REFERENCES

Bolton (H. C.), Fawcett (W.), and Gurney (I. D. C.), 1962. *Proc. Phys. Soc.* **80**, 199.

Bragg (W. L.), 1924. *Proc. R. Soc.* **105**, 370.
Burns (R. G.) and Strens (R. G. J.), 1967. *Mineral. Mag.* **36**, 204.
Deer (W. A.), Howie (R. A.), and Zussman (J.), 1962. *Rock Forming Minerals*. London (Longmans), New York (Wiley).
Fawcett (W.) 1963a. 'Theoretical Studies on the Refractivities of Ionic Crystals.' Ph.D. Thesis, University of Newcastle upon Tyne.
—— 1963b. *Proc. Phys. Soc.* **82**, 33.
Freer (R.), 1973. 'The Optical Properties of Solid Solutions.' M.Sc. Thesis, University of Newcastle upon Tyne.
Gehlen (K. von) and Piller (H.), 1965. *Mining Mag.* **113**, 438.
Hartshorne (N. H.) and Stuart (A.), 1960. *Crystals and the Polarising Microscope*. London (Edward Arnold).
Jenkins (F. A.) and White (H. E.), 1976. *Fundamentals of Optics*. 4th edn, New York (McGraw-Hill).
Johnston (R. W.), 1949. *Mineral. Mag.* **28**, 505.
Kittel (C.), 1966. *Introduction to Solid State Physics*. 3rd edn, New York (Wiley).
Langer (K.), Abu-Eid (R. M.), and Anastasiou (P.), 1976. *Z. Kristallogr.* **144**, 434.
Mott (N. F.) and Gurney (R. W.), 1964. *Electronic Processes in Ionic Crystals*. New York (Dover).
Myer (G. H.), 1966. *Am. J. Sci.* **264**, 364.
Nitsan (U.) and Shankland (T. J.), 1976. *Geophys. J. R. Astron. Soc.* **45**, 59.
Partington (J. R.), 1953. *Advanced Treatise on Physical Chemistry*, **4**. *Physiochemical Optics*. London (Longmans).
Robbins (D. W.) and Strens (R. G. J.), 1972. *Mineral. Mag.* **38**, 551.
Smith (G.) and Strens (R. G. J.), 1976. *In* Strens (R. G. J.), ed. *The Physics and Chemistry of Minerals and Rocks*. London & New York (Wiley).
Strens (R. G. J.), 1967. *Mineral. Mag.* **35**, 928.
Tossell (J. A.) and Vaughan (D. J.), 1974. *Am. Mineral.* **59**, 319.
Wood (B. J.), 1971. 'Electronic Spectra of some Solid Solutions.' Ph.D. Thesis, University of Newcastle upon Tyne.
—— and Strens (R. G. J.), 1970. Abstracts, IMA–IAGOD Meeting (Tokyo), 116.
—— —— 1972. *Mineral. Mag.* **38**, 909.
Wooster (W. A.), 1931. *Z. Kristallogr.* **80**, 495.